Nonlinear Mach-Zehnder-Fano interferometer

Andrey E. Miroshnichenko and Yi Xu
Nonlinear Physics Centre and Centre for Ultra-high bandwidth Devices for Optical Systems (CUDOS),
Australian National University, Canberra ACT 0200, Australia
Email: aem124@physics.anu.edu.au

***Abstract*— We consider nonlinear Mach-Zehnder-Fano interferometer in which supports the nonlinear Fano resonances. Based on the introduced figure of merit, we demonstrate that the nonlinear Mach-Zehnder-Fano interferometer could enhance the nonlinear response up to two orders of magnitude and produce the nearly perfect dynamical bistable response compared to standard Fano resonance geometry. The enhanced resonance excitation in the nonlinear Fano defect and the step-function like linear transmission suggest that the Mach-Zehnder-Fano interferometer could be a suitable candidate involving in nonlinear manipulation of the Fano resonance. We confirm the significant enhancement of the nonlinear sensitivity both in stationary and dynamic manners. We further suggest a nonlinear photonic crystal circuit as one of the possibilities to realize our results.**

I. Introduction

Mach-Zehnder interferometer (MZI) is a key component in many branches of physics due to its capacity of manipulating the coherent signal [1]. By coupling a cavity to the MZI may further facilitates the engineering of the coherent phase sensitivity. Enhanced all-optical switching and bistability had been demonstrated in a ring-resonator-coupled Mach-Zehnder interferometer which exactly shows the potential for effective and coherent control of the nonlinear resonator. Recently, we have introduced the concept of Mach-Zehnder-Fano interferometer (MZFI) [4] which offers the opportunity to manipulate the interaction of Fano resonances. The MZFI has unique physical properties which can not been found in the macroscopic resonator enhanced MZI. Furthermore, due to the small defect volume compared with the macroscopic resonator, the counterpart of the ring-resonator-coupled Mach-Zehnder interferometer in the microscopic scale, i.e. MZFI constructed by PhCs seems to be more promising for future application.

As one of the key features of the nonlinear Fano resonance, bistability received increasing attention especially in the optical society. With the advantage of compact in size and the state-of-the-art fabrication technology [5], Photonic crystals (PhCs) based bistable type optical switching received tremendous research attention these years [6], [7], [8], [9], [10], [11], [12], [13], [14], [15], [16], [17]. The manifest optical bistable state can be treated based on the simple model of the nonlinear Fano resonance [19], [20]. By suitable engineering the asymmetric degree of the linear Fano resonance one has the opportunity to access the high extinction ration, large modulation depth and low power nonlinear switching [21], [22].

The aim of this paper is to explore the nonlinear physical properties of the MZFI which can be outlined by the enhanced nonlinear response and the dynamic bistability. The nonlinear MZFI involves nonlinear Fano defect which would in turn act as a nonlinear scttering potential in the arms of the MZI. We study both the stationary and transient response of the system based on the modified Fano-Anderson model [19]. To check the validity of our results, we consider a nonlinear PhCs circuit to support our theoretical proposal.

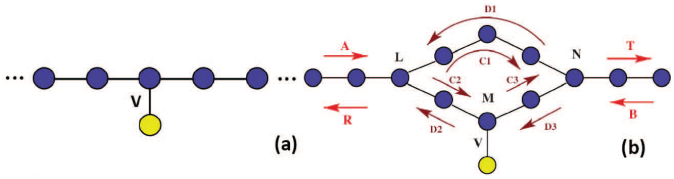

Fig. 1. (a) and (b) are the generic discrete models for the system exhibiting Fano resonance. Note that in the calculation, $E_d = 0, M = 4$, $L = 1$ and $N = -7$.

II. Model

We consider a generic discrete model [23] which can describe the dynamic of MZFI. The sketch map of two particular geometries are shown by Fig. 1 (a) and (b). By using the modified Fano-Anderson model, the equations of motion describing the system of Fig. 1 (b) are read as coupled discrete nonlinear equations:

$$\begin{aligned} i\dot{\psi}_n &= \textstyle\sum_k \quad \psi_k + \delta_{n,M} V \varphi_d \\ i\dot{\varphi}_d &= \quad E_d\varphi_d + \lambda|\varphi_d|^2\varphi_d + V\psi_M \ , \end{aligned} \tag{1}$$

where ψ_n represents the linear chain with complex field amplitude, φ_d stands for the Fano defect, M gives the location of the Fano defect in the arm, k is the total number of the neighbour sites in the chain, λ is the cubic nonlinear parameter, V is the coupling strength between the chain and the Fano defect, E_d is the eigenfrequency of the Fano defect and we assume the coupling between neighbouring sites C equal to unity.

For a specified case, the cavity-waveguide system supported by PhCs can be mapped to a similar discrete model [13]. The coupled nonlinear set of equations describes the dynamics of the PhCs based nonlinear MZFI.

The transmission properties of the system in the linear region can be found by solving a set of linear equations.

978-1-4577-0479-6/11/$26.00 ©2011 Crown

Fig. 2 (a) are the transmissions of the MZFI with two coupling symmetries, respectively. The detail parameters can be found in the caption. The standard Fano resonance case (Fig. 1 (a)) is shown by dotted line as a reference. It can be seen from the figures that the excitation of the Fano defects is distinct with different coupling symmetry. When the Fano defect locates at $M = 4$ in the arm, the transmission in the band centre looks like a step function. At the same time, the hybrid resonances have the highest defect excitation among these resonances because they are induced by the interaction of two Fano resonances. Intuitively, the high contrast step function like transmission as well as high resonant excitation in the nonlinear defect are positive factors for enhancing nonlinear response. We thus look into the nonlinear response of the system (2) at these specified resonances.

The stationary nonlinear switching is shown by the lines in Fig. 2 (c). We compare four kind of resonances marked ω_{a-d} at Fig. 2 (a). In order to compare the nonlinear response of the resonances, all of them start exactly at each of the completed transmission dip. As can be seen from the figures, the resonances with higher nonlinear defect excitation and more asymmetric linear transmission are corresponding to faster raising of transmission. It should be pointed out that the maximum of the defect excitation is in between the transmission dip and tip of such sharp and asymmetric lineshape. The excitation of resonance ω_d is mediated by the highly excitation of the site coupled with the Fano defect and it is *not* the eigenfrequency of the Fano defect. The resonance ω_d obtains nonlienar feedback only from its host (i.e. the nonlinear Fano defect). Therefore, ω_a involving with the eigen-frequency of the Fano defect would be more sensitive to the nonlinearity as shown by Fig. 2 (c). At the same time, the nonlinear response of ω_a is greatly reduced by the step function like linear transmission compared to resonance ω_b and ω_c. If we define a figure of merit(FOM) as T_{max}/P_{in}, where T_{max} refers to the nearest transmission maximum and P_{in} represents the necessary input power to pull the response of the system up to 90% of the T_{max}. The FOM of resonance ω_a, which describes both the enhanced transmission contrast in the linear case and the reduction of the switching power, can be enhanced as much as 67 times comparing to a given defect supporting standard Fano resonance ω_b [20]. The raising properties of the resonance ω_b and ω_c are similar because they are originated from the eigen-frequency of the Fano defect and are excited almost the same.

The dynamic nonlinear responses of the system at specified resonances are obtained by a pulse with $I = I_0 exp(-(T - T_0)^2/W^2)\sin(\omega t)$, where W is the pulse width, ω is set at the same frequencies with ω_{a-d}. Compared to the stationary one, the dynamic solution predicts similar nonlinear response except for the case of ω_a. We can see a unique properties that the transmission of resonance ω_a defuses above certain threshold of the input power as is indicated by the pink shaded region. This is caused by the dynamic and instability of the Fano resonance [24]. It should be noted that the width of the instability area and the transmission value is depended on the

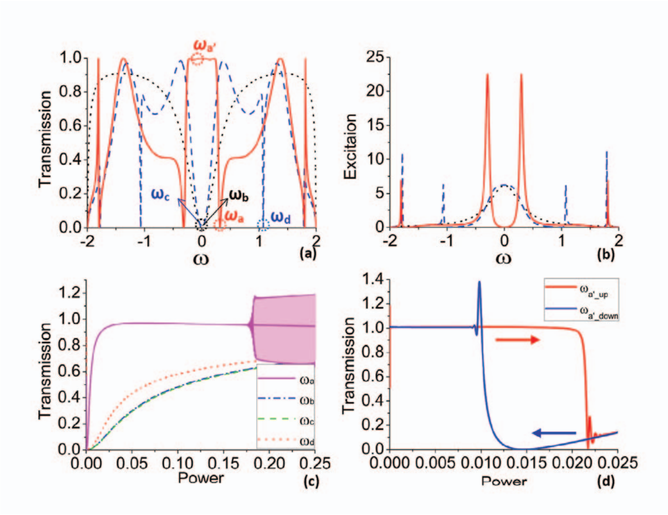

Fig. 2. (a) and (b) are the transmission and the excitation of the linear MZFI, respectively. (c) nonlinear response of different resonances marked ω_{a-d} at Fig. 2 (a). Lines present the stationary result of the system. Pink solid line stands for the hybrid Fano resonance marked ω_a in Fig. 2 (a), red dotted line presents the resonance of the MZI's loop marked ω_d while green dashed line and blue dashed-dotted lines represent the cases of eigen-Fano resonance of the Fano defect coupling to the MZI(marked ω_c) and coupling to a chain(marked ω_b), respectively. The pink shaded region represents the area of the dynamic modulational instability initialled by a pulse of $T_0 = 1.3 \times 10^4$, $W = 5 \times 10^3$ and $I_0 = 0.25$. (d) A typical bistability at the frequency $\omega = -0.21$ with respect to $\omega_{a'}$. Here, $T_0 = 1.3 \times 10^4$, $W = 5 \times 10^3$ and $I_0 = 0.025$. Red line and the blue line stand for the upward and downward nonlinear Fano bistable states.

properties of the excited pulse. The transmission is not well defined in the pink shaded region. We also notice that there is similar properties with the generic instability in the localized nonlinear system where the dynamic nonlinear process suffers from modulational instability. As had been pointed out by one of the authors A. E. Miroshnichenko that the continuum wave (CW) feeding to such system would induce time dependent exponential growing of the Fano defect's excitation at the vicinity of the nonlinear Fano resonance [24]. Such kind of divergence in time would make the system transfer to a transparent state rather than the resonant blocking when one intends to access the nonlinear Fano resonance by CW. Therefore the bistable operation would be strongly affected. Please note that all of the resonances have similar dynamic instabilities. Only the instability of ω_a appearing in Fig. 2 (c) is also an evidence of enhanced nonlinear response.

III. Photonic Crystal based nonlinear Mach-Zehnder-Fano interferometer

Using the modified Fano-Anderson model, we have proved that the nonlinear MZFI pronounces itself as a suitable candidate to realize the enhanced nonlinear response and the enhanced dynamic bistability. We thus suggest a PhCs platform as a specified possibility to realize the idea while the upper result can be applied to other kinds of similar discrete system. The PhCs structure is outlined by Fig. 3 (b). The PhCs is consisted by square dielectric rods suspending in air with the radius $r = 0.19a$,a is the lattice constant and

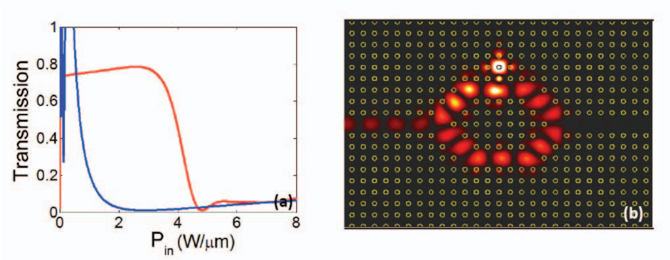

Fig. 3. (color online)(a) Bistable operation obtain by pulse excitation in nonlinear FDTD experiment. (b)electric field distribution ($|E|^2$) at the upward dynamic switching point.

the refractive index n is 3.14. A complete bandgap within the frequency range $0.316 - 0.445\ 2\pi a/c$ is supplied by the infinite PhCs. The arms of the MZFI is created by removing certain rods while the side couple nonlinear Fano defect is made by replacing one rod with a polymer rod($n = 1.59$) which supports a quadrupole mode at $f \approx 0.3723\ 2\pi c/a$. The third-order nonlinearity susceptibility of the polymer is $1.14 \times 10^{-12} cm^2/W$. We use the nonlinear Finite Difference Time Domain (FDTD) method which exactly solves the Maxwell equations to fully model the realistic problem. The bistable state shown in Fig. 3 (a) is obtain by the pulse with input frequency $f = 0.373\ 2\pi c/a$ and duration 30 picoseconds. The profile is similar with the theory except for the transmission of the on-state. Fig. 3 (b) shows the transient electric field distribution ($|E|^2$) at exactly the downward dynamic switching point(from on to off-state). Nearly perfect blocking of the input pulse demonstrates the dynamic shutting down operation by a pulse and successfully suppression of the modulation instability. The high excitation both in the Fano defect and the loop is also the signature of the hybrid Fano resonance in the MZFI. The reduction of the on-state transmission is caused by the reduction in the linear transmission and the transient shift of the defect mode [25]. Increasing the linear transmission can be done by careful designing which locates the interaction between the eigen-Fano resonance and the loop's resonance exactly at the band center. It should be pointed out that the discrete nonlinear MZFI is not limited to the PhCs case which presents a schematic example of nonlinear MZFI. And it can be generalized to fully describe the dynamics of other similar nonlinear system.

IV. Conclusion

In conclusion, we have discussed the nonlinear concept of the Mach-Zehnder-Fano interferometer. Both stationary and dynamic solutions convince the superiority of the enhanced nonlinear response and bistability in MZFI. The enhanced excitation in the nonlinear Fano defect and the asymmetry and high contrast linear transmission are the key reason that the MZFI would be benefited from the nonlinearity. Direct numerical simulations in two-dimensional PhCs confirm the theoretical prediction of the dynamic characteristics. The effective discrete model is general and can be applied to other branches of discrete physical system.

Acknowledgment

The authors thank Prof. Yuri Kivshar for useful discussions. A. E. Miroshnichenko was supported by the Australian Research Council. Y. Xu acknowledges the support from the China Scholarship Council and the Nonlinear Research Centre at ANU for their hospitality.

References

[1]
[2] John E. Heebner, Nick N. Lepeshkin, Aaron Schweinsberg, G. W. Wicks, Robert W. Boyd, Rohit Grover, and P.-T. Ho, Opt. Lett. **29**, 769-771 (2004).
[3] Ying Lu, Jianquan Yao, Xifu Li, and Peng Wang, Opt. Lett. **30**, 3069-3071 (2005).
[4] A. E. Miroshnichenko and Yu. S. Kivshar, Appl. Phys. Lett. **95**, 121109 (2009).
[5] Y. Akahane, T. Asano, B. S. Song, and S. Noda, Nature, **425**, 944 (2003).
[6] S. F. Mingaleev and Yuri S. Kivshar J. Opt. Soc. Am. B **19**, 2241-2249 (2002).
[7] M. Soljai, M. Ibanescu, S. G. Johnson, Y. Fink, and J. D. Joannopoulos, Phys. Rev. E **66**, 055601 (2002).
[8] M. F. Yanik, S. Fan, and M. Soljacic, Appl. Phys. Lett. **14**, 27392741 (2003).
[9] M. Soljai, C. Luo, J. D. Joannopoulos, and S. Fan, Opt. Lett. **28**, 637-639 (2003).
[10] T. Tanabe, M. Notomi, S. Mitsugi, A. Shinya, and E. Kuramochi, Opt. Lett. **30**, 2575-2577 (2005).
[11] M. Notomi, A. Shinya, S. Mitsugi, G. Kira, E. Kuramochi, and T. Tanabe, Opt. Express **13**, 2678-2687 (2005).
[12] Bjrn Maes, Peter Bienstman, and Roel Baets, J. Opt. Soc. Am. B **22**, 1778-1784 (2005).
[13] S. F. Mingaleev, A. E. Miroshnichenko, Yu. S. Kivshar, and K.Busch, Phys. Rev. E **74**, 046603 (2006).
[14] S. F. Mingaleev, A. E. Miroshnichenko, and Yu. S. Kivshar, Opt. Express **15**, 12380-12385 (2007).
[15] S. F. Mingaleev, A. E. Miroshnichenko, and Yu. S. Kivshar, Opt. Express **16**, 11647-11659 (2008).
[16] S. H. Li and X. H. Cai , Appl. Phys. Lett. **96**, 131114 (2010).
[17] S. Sandhu, M. L. Povinelli, and S. Fan Appl. Phys. Lett. **96**, 231108 (2010).
[18] U. Fano, Phys. Rev. **124**, 1866 (1961).
[19] A. E. Miroshnichenko, S. Flach, and Yu. S. Kivshar, Rev. Mod. Phys. **82**, 2257 (2010).
[20] A. E. Miroshnichenko, S. F. Mingaleev, S. Flach, and Yu. S. Kivshar, Phys. Rev. E **71**, 036626 (2005)
[21] S. Fan, Appl. Phys. Lett. **80**, 908-910 (2002).
[22] L. Y. Mario, S. Darmawan, and Mee K. Chin, Opt. Express **14**, 12770-12781 (2006).
[23] A. E. Miroshnichenko, M. I. Molina, and Yu. S. Kivshar, Phys. Rev. E **75**, 046602 (2007).
[24] A. E. Miroshnichenko, Yu. Kivshar, C. Etrich, T. Pertsch, R. Iliew, and F. Lederer, Phys. Rev. A **79**, 013809 (2009).
[25] X. S. Lin, Q. Shi, X. H. Cai, N. S. Zhao, and S. Lan, Opt. Express **14**, 6794-6799 (2006).
[26] A. Arnold, M. Ehrhardt, I. Sofronov, Commun. Math. Sci. **1**, 501 (2003).